arXiv:2510.23688v1 [physics.soc-ph] 27 Oct 2025

Collective Motion from Quantum-Inspired Open Dynamics with Self–Perception Coupling: A Bloch Approximation Framework

Jyotiranjan Beuria

IKS Research Centre, ISS Delhi, Delhi, India

October 29, 2025

Abstract

In cognition, the perception of external stimuli and the self-referential awareness of one's own perceptual process are two distinct but interacting operations. We propose a quantum–inspired framework in which both the self state and the perception state are treated as coupled open quantum systems evolving across two different timescales. The fast perceptual subsystem captures adaptive sensing under coherent and dissipative influences, while the self subsystem evolves on a slower timescale, integrating perceptual feedback into a stable internal state. Their mutual coupling forms a closed informational loop, where the self-state biases perception, and perception continually reshapes the self. A macroscopic collective order emerges from the interplay of feedback, dissipation, and coherence. Although the Lindblad formalism rigorously captures microscopic quantum dynamics, the Bloch representation offers a far more tractable and intuitive description by compressing the evolution into observable quantities such as polarization, alignment, and coherence decay. Within this framework, we further identify several meaningful dynamical indicators, such as the collective order parameter, the degree of self-coherence, and the volitional inertia inferred from hysteresis-like loops, which together provide a quantitative characterization of emergent coordination and adaptation in a self-perception coupled system. Unlike traditional models of active matter that rely on instantaneous interaction rules, the introduction of an internal, slow-evolving self-subsystem integrates the history of perceptual interactions to capture adaptive and memory-dependent behavior.

1 Introduction

Collective motion is one of nature's most striking examples of self-organization [1–3]. From bird flocks [4] and fish schools [5] to pedestrian crowds [6, 7], neural populations [8], and distributed robotic swarms [9], coordinated movement emerges without a centralized controller, guided only by local interactions among autonomous agents. Understanding how such collective coordination arises has been an enduring scientific challenge, linking statistical physics, control theory, neuroscience, and cognitive science.

Classical models of collective motion, such as the Vicsek model [10] or Toner-Tu model [11], describe agents as self-propelled particles aligning their direction of motion with neighbours under stochastic perturbations. These models successfully capture phase transitions between disordered and ordered movement but treat each agent as a simple reactive unit with

no internal cognitive dynamics. Similarly, associative-memory and Ising-like formulations of collective decision-making have modelled collective coordination [12], but cannot account for dynamic uncertainty, interference, or contextual modulation that characterise real perceptual and cognitive processes.

Human decision-making rarely follows the neat prescriptions of classical probability or rational-choice theory [13, 14]. Empirical studies consistently show contextuality, order effects, interference of alternatives, and hesitation between incompatible choices [14–16]. These are the signatures of a process that is dynamic and uncertain. When faced with ambiguity, individuals often maintain superposed mental states, holding competing intentions or evaluations simultaneously before one outcome crystallizes through reflection, attention, or social influence. Traditional stochastic or Bayesian models cannot fully capture this fluid interplay between coherence, uncertainty, and contextual modulation.

In recent years, quantum-inspired models of cognition [17–19] have introduced a powerful new paradigm for understanding decision-making and collective behavior. These approaches are termed quantum-like or quantum-inspired because they employ the mathematical formalism of quantum mechanics to model cognitive processes, without implying that actual quantum phenomena occur in the brain [20]. By representing cognitive states as evolving vectors in Hilbert space, such models naturally capture key features of human cognition, including superposition (coexisting intentions), interference (contextual modulation of preference), and entanglement (coupling between beliefs, emotions, and social cues) [14, 16].

In our recent work [19], we extended this framework to collective motion by representing each agent's perceptual state as a superposition of alternative choices, i.e., to follow or not follow a neighbor, and showed that macroscopic coordination emerges from the expectation values of a perception operator, recovering classical flocking dynamics as a limiting case. These developments highlight the broader potential of quantum-inspired modeling to describe systems where coherence, contextuality, and interaction shape emergent order. However, real cognitive and collective systems are inherently open: they continuously exchange information and influence with their surroundings. Decision-making, in particular, reflects an open-system process [18,21,22], in which internal deliberation and environmental feedback jointly drive the transition from potentiality to action. Thus, a comprehensive foundation for collective motion requires not only an open quantum–inspired framework, but one that unifies self-regulation, perception, and collective adaptation within a single dynamical model.

While quantum-inspired models successfully capture perceptual uncertainty and contextual decision processes, they primarily address the dynamics of perception and choice without adequately accounting for the agent's capacity for self-regulation or intentional control. These models describe perceptual and decisional states as evolving quantum states in Hilbert space, capable of exhibiting superposition, contextuality, and interference, which are the features that mirror human cognition. However, a fundamental ingredient of cognition is still missing from such perception-only models, namely, the self. The notion of the self is a nuanced construct encompassing philosophical, psychological, phenomenological, and neural dimensions [23, 24]. In the proposed framework of this work, the self is not treated as a metaphysical entity but as an internal regulatory subsystem that integrates information over longer timescales, modulates perceptual dynamics, and provides a source of volitional stability within the agent. Perception alone cannot explain volition, sustained attention, or the ability of agents to regulate their own perceptual field, which is a hallmark of active or self-propelled agents.

Empirical studies in cognitive neuroscience indicate that self-referential integration arises from large-scale interactions among cortical midline structures [25–27], notably the medial prefrontal cortex and posterior cingulate cortex, which form part of the brain's intrinsic or

default-mode network [27, 28]. From a dynamical-systems viewpoint, such regions operate as slow integrative nodes [29] that maintain internal reference states and modulate perceptual processing through recurrent feedback loops. In this sense, the self may be understood as an internal regulatory degree of freedom that stabilizes perception by providing a long-timescale context or bias field. However, existing quantum-inspired models of cognition and collective behavior rarely include a self-referential component, which is essential for top-down modulation and adaptive control within an open-system framework, where active agents remain in continuous interaction and information exchange with their environment.

In the proposed framework, each agent is represented by two interacting open quantum [30, 31] subsystems: a self qubit and a perceptual qubit for each neighbor. The self qubit encodes the agent's internal volitional or attentional state. In contrast, each perceptual qubit represents the agent's decision state with respect to a neighbor or an environmental cue. The self and perceptual subsystems are coupled bidirectionally: the self modulates how perceptual superpositions collapse into choices, while perceptual outcomes continuously update the self through feedback. This coupling forms an open quantum system that exchanges information with its surroundings, allowing both internal regulation and collective adaptation to emerge from the same dynamical process.

We perform detailed numerical simulations considering the Bloch approximation. It reveals (i) the existence of distinct time scales at self and perceptual levels; (ii) self-coherence has an essential impact on collective order; (iii) hysteresis and memory effects indicating persistence of volitional bias; and (iv) leaderless synchronisation, where groups spontaneously coordinate without explicit leadership. Together, these results suggest that collective motion is not only a product of perceptual coupling but also of a self-modulated process.

The organization of this work is as follows. In section 2, we lay down the framework considering full open quantum system dynamics and its Bloch approximation. In section 3, we define several observables for this framework. We present results from detailed numerical simulations in section 4 and finally we conclude in section 5.

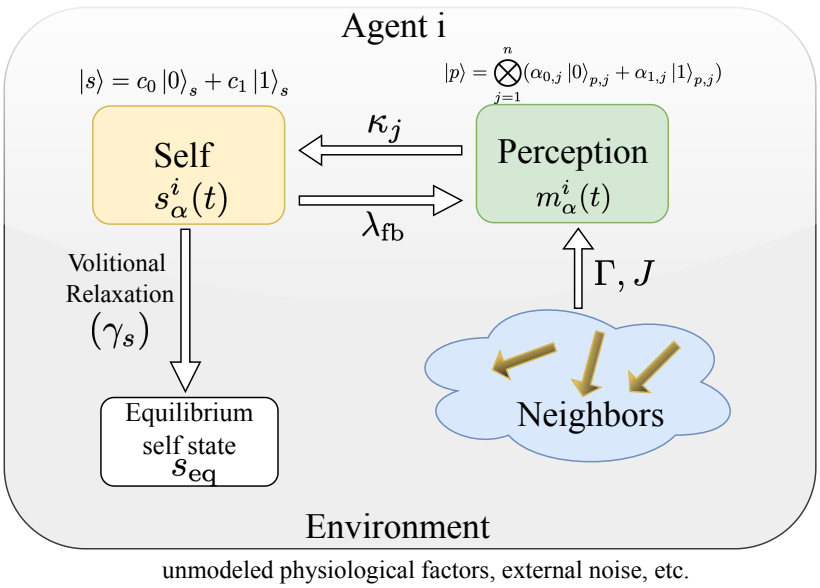

Figure 1: Self-Perception interaction framework that leads to macroscopic alignment and collective motion.

2 The Framework

We consider N active agents that interact via perceptual mechanisms such as vision in the case or birds. Through the interplay of perception mechanism and individual decision to align with a set of randomly chosen neighbors, an ordered pattern emerges. We wish to formulate a quantum-inspired framework to describe the coexistence and continual fluctuation of perceptual and self states within each agent that eventually leads to coordinated behavior. We represent both the perceptual and self subsystem as an effective two–level quantum system. The perceptual state of an active agent is represented by its decision to follow a neighbor or not. Since there are multiple neighbors of an agent at a given instant of time, its perceptual state can be modeled using a superposition of all these binary decision states. In other words, $|1\rangle_p$ and $|0\rangle_p$ represent a decision to follow a neighbor or not, respectively. Similarly, the self subsystem encodes the agent's internal volitional or attentional state. Its basis states correspond to $|1\rangle_s$: self-excitation, attentional focus, and volitional engagement, and $|0\rangle_s$: self-inhibition, passive response, or low self-modulation. These two subsystems together characterize the cognition of the active agent. In this proposed framework, we primarily consider that the cognition of every agent is independent. Thus, one common neighbor can contribute to the perceptual state of different agents differently. A schematic diagram for this framework is shown in figure 1.

Because each agent continuously exchanges perceptual and behavioral information with its neighbors and the surrounding physical environment, its cognitive state cannot be regarded as an isolated quantum system. The perceptual subsystem is driven by fluctuating external stimuli and neighboring cues, while the self subsystem experiences internal dissipation and stochastic modulation due to noise, fatigue, or other unmodeled physiological factors. Together, these interactions constitute an effective environment that induces decoherence and relaxation of the agent's cognitive state. Consequently, the joint perceptual–self state of an agent is best described as an open quantum system, whose reduced density operator $\rho_i(t)$ evolves according to the Gorini–Kossakowski–Sudarshan–Lindblad (GKSL) master equation [30, 31],

$$\dot{\rho}_i = -i[H_i, \rho_i] + \sum_k \mathcal{D}[L_{k,i}]\rho_i, \tag{1}$$

where H_i encodes coherent perceptual–self coupling and $\mathcal{D}[L_{k,i}]$ are dissipators representing interaction with the environment. Next, we describe the evolution of this open quantum system and its Bloch approximation.

2.1 Complete GKSL formulation

The coupled dynamics of perception and self subsystems within a single agent i, can be modeled as a composite open quantum system Hilbert space $\mathcal{H}_i = \mathcal{H}_{s,i} \bigotimes_{j=1}^{n} \mathcal{H}_{p,j}$, where $\mathcal{H}_{s,i}, \mathcal{H}_{p,j} \simeq \mathbb{C}^2$ represent the two–level self qubits and n is the number of neighbors for agent i. The Hamiltonian for every agent is decomposed as

$$H = H_s + H_p + H_{sp} + P(X(t)), \tag{2}$$

with intuitive roles as follows (:

$$H_s = -\Gamma_s S_x - J_s S_z, \qquad \text{(intrinsic self-precession)} \tag{3}$$

$$H_p = -\Gamma \sum_{j=1}^{n} \sigma_x^{(j)} - \sum_{k<j} J_{jk}\, \sigma_z^{(j)} \sigma_z^{(k)}, \qquad \text{(perceptual alignment and coupling)} \tag{4}$$

$$H_{sp} = -\sum_{j=1}^{n} \kappa_j\, S_z \otimes \sigma_z^{(j)}, \qquad \text{(self–perception interaction)} \tag{5}$$

$$P(X) = -\sum_{j=1}^{n} h_j(X)\, \sigma_z^{(j)}, \qquad \text{(external sensory drive).} \tag{6}$$

Here, Γ_s and Γ control intrinsic rotations in the self and perceptual subspaces, J_{jk} represents mutual alignment among perceptual qubits, and κ_i quantifies how strongly the agent's self bias (S_z) couples to each perceptual channel $\sigma_z^{(j)}$. The external term $P(X)$ represents time-dependent sensory inputs or environmental cues. Together, these contributions describe how the agent's internal state precesses coherently under self, perceptual, and environmental influences.

Environmental noise and interaction with other agents introduce decoherence and relaxation, encoded by the Lindblad dissipator

$$\mathcal{D}[\rho] = \sum_{\alpha} \gamma_\alpha \Big(L_\alpha \rho L_\alpha^\dagger - \tfrac{1}{2}\{L_\alpha^\dagger L_\alpha, \rho\} \Big), \tag{7}$$

where each operator L_α represents a specific physical or cognitive noise process acting locally on the perceptual or self subsystem. The minimal, physically motivated channels used here are:

- **Perceptual dephasing:** $L_i^{(\phi)} = \sqrt{\gamma_\phi}\, I_s \otimes \sigma_z^{(i)}$. This models random phase fluctuations, i.e., loss of perceptual coherence without population transfer, which is analogous to sensory noise or fluctuating attention. It preserves populations but exponentially suppresses off-diagonal terms ($\rho_{01} \to \rho_{01} e^{-2\gamma_\phi t}$), defining the transverse timescale T_2.

- **Perceptual amplitude damping:** $L_i^- = \sqrt{\gamma_-}\, I_s \otimes \sigma_-^{(i)}$ (and L_i^+ with rate γ_+). These represent energy-exchange processes that drive perceptual decisions toward stable outcomes, yielding population relaxation ($\dot{\rho}_{11} = -\gamma_- \rho_{11} + \gamma_+ \rho_{00}$) and contributing to longitudinal relaxation time T_1.

- **Self relaxation:** $L_s^- = \sqrt{\gamma_s}\, S_- \otimes I_P$. This induces slow decay of the self's longitudinal component s_z, capturing the gradual relaxation of volitional or attentional engagement over timescale $1/\gamma_s$.

These channels together ensure trace preservation and complete positivity while capturing the essential physical picture: the self–perception system is continuously driven, decohered, and relaxed by its environment. The GKSL formalism provides a unified and thermodynamically consistent framework for describing such open dynamics. When expressed in terms of the expectation values of the Pauli observables, the GKSL equation reduces to coupled real-valued Bloch equations governing the evolution of (m_x, m_y, m_z) and (s_x, s_y, s_z). This Bloch approximation retains all relevant phenomenology, namely, precession, decoherence, and relaxation, while offering a computationally efficient description scalable to ensembles of hundreds of interacting agents.

2.2 Bloch reduction: deriving mean-field ODEs from the Lindblad equation

Under the weak-coupling and Markovian approximations, the expectation values of the Pauli observables $m^i_\alpha(t) = \mathrm{Tr}(\sigma^i_\alpha \rho_i)$ for $\alpha \in \{x, y, z\}$ evolve according to real-valued Bloch equations. These equations provide a reduced, geometric representation of each agent's quantum-inspired cognitive state, capturing precession, relaxation, and feedback in a three-dimensional phase space. This Bloch description offers two key advantages: (i) It gives an intuitive geometric interpretation, where each agent's state corresponds to a point on or inside the Bloch sphere. The longitudinal alignment m_z encodes the dominant perceptual choice (e.g., follow vs. not follow), while the transverse components (m_x, m_y) measure coherence between these alternatives; and (ii) It enables efficient simulation of large collectives, since one evolves simple coupled ordinary differential equations for (m^i_x, m^i_y, m^i_z) instead of exponentially large density matrices.

Mean-field factorization. To obtain a scalable description for many interacting agents, we adopt the standard mean-field product ansatz:

$$\rho(t) \approx \rho_s(t) \otimes \bigotimes_{j=1}^{n} \rho_j(t),$$

where ρ_s is the self-qubit's reduced state and ρ_j is the reduced density matrix of perceptual qubit j. Each single-qubit density matrix admits the Bloch form

$$\rho_i = \tfrac{1}{2}\big(I + \mathbf{m}_i \cdot \boldsymbol{\sigma}\big), \qquad \rho_s = \tfrac{1}{2}\big(I + \mathbf{s} \cdot \mathbf{S}\big), \tag{8}$$

with corresponding Bloch vectors $\mathbf{m}_i = (m^i_x, m^i_y, m^i_z)$ and $\mathbf{s} = (s_x, s_y, s_z)$. The dynamical equations for these components follow from

$$\dot{m}^i_\alpha = \mathrm{Tr}\big(\sigma^{(i)}_\alpha \dot{\rho}\big), \qquad \dot{s}_\alpha = \mathrm{Tr}\big(S_\alpha \dot{\rho}\big).$$

Unitary precession. For a single-site effective Hamiltonian

$$H^{(i)}_{\text{eff}} = -\Gamma\, \sigma^{(i)}_x - h^{\text{eff}}_i\, \sigma^{(i)}_z,$$

the commutator term $-i[H, \rho]$ in Eq. (1) yields

$$\mathrm{Tr}\big(\sigma^{(i)}_\alpha [-iH^{(i)}_{\text{eff}}, \rho_i]\big) = 2(\mathbf{B}_i \times \mathbf{m}_i)_\alpha,$$

with the effective magnetic field $\mathbf{B}_i = (-\Gamma, 0, -h^{\text{eff}}_i)$. This cross product describes coherent precession of the perceptual Bloch vector around $\mathbf{B}_i$, analogous to perceptual oscillations or alternating dominance between choices.

Dissipative relaxation. The dissipator $\mathcal{D}[\rho]$ in Eq. (1) introduces decoherence and population relaxation. Local pure-dephasing channels $L^{(\phi)}_i = \sqrt{\gamma_\phi}\, \sigma^{(i)}_z$ cause exponential decay of the transverse components (m_x, m_y) at rate $2\gamma_\phi$, modeling the loss of coherent competition between perceptual alternatives (e.g., attentional fluctuations). Amplitude-damping channels

$L_i^- = \sqrt{\gamma_-}\,\sigma_-^{(i)}$ drive longitudinal relaxation of m_z with rate $\gamma_- + \gamma_+$, corresponding to stabilization of a perceptual choice or decision. These processes are parameterized by the phenomenological relaxation times T_1 and T_2, related by the standard expression

$$\frac{1}{T_2} = 2\gamma_\phi + \frac{1}{2T_1}.$$

Here, T_1 sets the timescale for perceptual reorientation, while T_2 controls the persistence of perceptual coherence.

Perceptual Bloch equations. Combining the unitary and dissipative contributions yields the mean-field Bloch equations for each perception subsystem:

$$\dot{m}_x^i = 2h_i^{\text{eff}}\, m_y^i - \frac{m_x^i}{T_2}, \tag{9a}$$

$$\dot{m}_y^i = -2h_i^{\text{eff}}\, m_x^i + 2\Gamma\, m_z^i - \frac{m_y^i}{T_2}, \tag{9b}$$

$$\dot{m}_z^i = -2\Gamma\, m_y^i - \frac{m_z^i - m_z^{\text{eq}}(h_i^{\text{eff}})}{T_1}, \tag{9c}$$

where the effective longitudinal field incorporates environmental, social, and self influences:

$$h_i^{\text{eff}}(t) = h_i(X(t)) + \sum_j J_{ij}\, m_z^j(t) + \kappa_i\, s_z(t). \tag{10}$$

The equilibrium magnetization $m_z^{\text{eq}}(h) = \tanh(\beta h)$ arises from detailed-balance properties of amplitude-damping channels, with β representing an effective inverse temperature. Equation (9) thus captures how each agent's perceptual state evolves and relaxes under the combined influence of external stimuli, local alignment, and the slow self subsystem.

Self Bloch equation (slow dynamics). In addition to the fast perceptual Bloch vectors (m_x^i, m_y^i, m_z^i) for each neighbor, each agent possesses a slow adaptive self variable s_i that integrates internal relaxation with feedback from its perceptual neighborhood. Its dynamics are modeled phenomenologically as

$$\dot{s}_i = -\gamma_s\,(s_i - s_{\text{eq}}) + \lambda_{\text{fb}}\,\langle m_z\rangle_{\text{neigh}}, \tag{11}$$

where $\gamma_s > 0$ determines the intrinsic rate of return to equilibrium s_{eq}, and λ_{fb} quantifies the feedback strength from the mean longitudinal perceptual alignment of nearby agents, $\langle m_z\rangle_{\text{neigh}}$. Equation (11) expresses a linear–response mechanism in which the slow self variable relaxes toward its baseline state while being driven by collective perceptual input. Its characteristic timescale γ_s^{-1} is much longer than those of the perceptual Bloch variables (T_1, T_2), establishing a natural slow–fast hierarchy in the model. The relation of microscopic Lindblad rates and phenomenological parameters is:

$$T_2^{-1} \approx 2\gamma_\phi + \tfrac{1}{2}(\gamma_- + \gamma_+), \qquad T_1^{-1} \approx \gamma_- + \gamma_+,$$

and the equilibrium bias satisfies $m_z^{\text{eq}} \approx (\gamma_+ - \gamma_-)/(\gamma_+ + \gamma_-) \approx \tanh(\beta h)$ for a thermalizing bath.

2.3 Action-Perception operators and mapping to physical motion

To couple internal perceptual variables to physical motion, we introduce action operators. A canonical, orientation-encoding operator for agent i is

$$\hat{O}_{A_i} = a\,(\sigma_x^{(i)} + i\sigma_y^{(i)}), \tag{12}$$

whose expectation

$$u_i(t) \equiv \langle \hat{O}_{A_i} \rangle = a\big(m_x^i(t) + i m_y^i(t)\big) \tag{13}$$

defines a complex heading. For simplicity, we choose $a = 1$. From our discussion on Bloch approximation, the natural choice for the perception operator becomes

$$\hat{O}_{P_i} = \sigma_z^{(i)}. \tag{14}$$

The physical velocity is then set by a mapping

$$\mathbf{v}_i(t) = v_0\, f(|u_i|)\, \hat{e}(\arg u_i), \qquad \hat{e}(\phi) = (\cos\phi, \sin\phi), \tag{15}$$

with f a nonnegative scaling function (for instance $f(r) = r$ or $f(r) = \frac{r}{r+r_0}$). This mapping generalizes the Vicsek alignment rule by deriving heading and speed directly from quantum expectation values. In our model, we choose $f(r) = r$ for simplicity.

3 The Observables

The dynamics of self-perception coupling can be studied at two complementary levels: the Bloch mean-field and the full Lindblad descriptions. The Bloch approach captures collective alignment, relaxation, and timescale separation between perception and volition, whereas the complete GKSL framework reveals detailed microscopic features characteristic of an open quantum system. Computationally, the GKSL formulation encompasses the Bloch dynamics as its mean-field limit, enabling both macroscopic and microscopic observables to be derived consistently. In this work, we focus on macroscopic properties involving a large number of agents; thus, we utilize the Bloch approximation method.

3.1 Bloch Mean Field related properties

3.1.1 Global order parameters

The collective alignment or perceptual coherence is measured by the mean-field order parameter

$$M(t) = \frac{1}{N}\left\| \sum_{i=1}^{N} \frac{u_i(t)}{|u_i(t)| + \varepsilon} \right\| \tag{16}$$

$$= \frac{1}{N}\left\| \sum_{i=1}^{N} \frac{m_{x,i}(t) + i m_{y,i}(t)}{|m_{x,i}(t) + i m_{y,i}(t)| + \varepsilon} \right\|, \tag{17}$$

analogous to the Vicsek order parameter in active matter models. $M(t) \approx 1$ corresponds to perfect alignment of headings, and $M(t) \approx 0$ represents completely random motion of agents. Each agent's self-state is characterized by the expectation value of its self qubit operator $\sigma_{z,i}$, i.e.,

$$s_i(t) = \mathrm{Tr}[\rho_{s,i}(t)\, \sigma_{z,i}]\,, \tag{18}$$

where $\rho_{s,i}(t)$ is the reduced density matrix of the ith agent's self subsystem, obtained by tracing over perceptual and environmental degrees of freedom. The quantity $s_i(t)$ thus represents the longitudinal polarization of the self, measuring its instantaneous degree of volitional engagement or internal regulation. Thus, we define the average self-tone as follows:

$$S(t) = \frac{1}{N}\sum_{i=1}^{N} s_i(t). \tag{19}$$

Positive values of the average self-tone, $S(t) > 0$, correspond to a population that is predominantly self-engaged, exhibiting strong volitional control, introspective regulation, and sustained attention. When $S(t) \approx 0$, the system occupies a mixed or neutral self-state in which agents fluctuate between internally driven and externally reactive modes. Negative values, $S(t) < 0$, denote a self-suppressed regime where perception dominates and internal regulation is weak, reflecting a predominantly reactive collective state.

In practice, the average self-tone $S(t)$ can be inferred from slow temporal patterns that reflect the degree of internal regulation or volitional engagement in the system under study. In neurocognitive settings, we hypothesize that $S(t)$ may correspond to low-frequency coherence or power fluctuations in cortical midline regions such as the medial prefrontal and posterior cingulate cortices, measurable via fMRI or EEG as markers of self-referential processing [29]. In behavioural collectives, it can be estimated from persistence or inertia in individual headings or decision trajectories, i.e., the tendency of an agent to maintain its own state before responding to neighbours. In robotic or artificial agents, $S(t)$ maps to the average feedback gain controlling self-stabilization versus neighbour influence. Across these domains, $S(t)$ thus quantifies the slow, internally generated component of regulation that biases fast perceptual dynamics, providing an empirically accessible signature of collective volitional tone.

The pair (M, S) defines a two-dimensional macroscopic state space that jointly characterizes the dynamics of perception and self-regulation.

3.1.2 Self-perception correlation and phase lag

The dynamical coupling between the perceptual and self subsystems is quantified by the normalized covariance

$$C_{MS} = \frac{\langle (M(t) - \bar{M})(S(t) - \bar{S})\rangle_t}{\sigma_M \sigma_S}, \tag{20}$$

where $\langle\cdot\rangle_t$ denotes temporal averaging over the observation window, $\bar{M}$ and $\bar{S}$ are time-averaged means of $M(t)$ and $S(t)$, and σ_M, σ_S are their corresponding standard deviations. The coefficient C_{MS} takes values in $[-1, 1]$: $C_{MS} \approx 1$ indicates strong positive entrainment between perception and self (i.e., high self–perception coherence), $C_{MS} \approx 0$ corresponds to weak or decoupled regimes, and $C_{MS} < 0$ signals anti-phase or opposing fluctuations.

A complementary measure of their temporal coordination is the instantaneous phase difference

$$\Delta\Phi_{MS}(t) = \arg[\tilde{M}(t)] - \arg[\tilde{S}(t)], \tag{21}$$

where $\tilde{M}(t)$ and $\tilde{S}(t)$ are the analytic signals obtained via the Hilbert transform, $\tilde{X}(t) = X(t) + i\,\mathcal{H}[X(t)]$, and $\mathcal{H}[\cdot]$ denotes the Hilbert operator. A positive $\Delta\Phi_{MS}$ indicates that changes in the self subsystem lag behind perceptual dynamics (reactive response), whereas a negative $\Delta\Phi_{MS}$ corresponds to anticipatory self modulation.

Together, C_{MS} and $\Delta\Phi_{MS}$ provide complementary insights into the coordination between fast perceptual fluctuations and slow self-regulatory dynamics: C_{MS} measures the strength of their statistical coupling, while $\Delta\Phi_{MS}$ reveals the direction and timing of their interaction.

3.1.3 Hysteresis and volitional inertia

To investigate the persistence and memory dynamics of the self-regulating field, we perform quasistatic sweeps of the feedback coupling parameter, denoted by λ_{fb}, which governs the strength of self-perceptual feedback. The parameter is slowly varied according to

$$\lambda_{\text{fb}}(t) : 0 \longrightarrow \lambda_{\text{fb}}^{\max} \longrightarrow 0,$$

while recording the stationary perceptual order parameter $M^*(\lambda_{\text{fb}})$ during both the forward (increasing) and backward (decreasing) phases of the sweep.

The resulting trajectories in the $(\lambda_{\text{fb}}, M^*)$ plane typically form a *hysteresis loop*, signifying that the system's current perceptual state depends not only on the instantaneous feedback strength but also on its prior self configuration. This history-dependent behavior indicates an intrinsic volitional inertia, where the self field exhibits resistance to abrupt perceptual realignment.

The corresponding loop can equivalently be visualized in the (S^*, M^*) state space, where the enclosed area,

$$\mathcal{A}_{\text{hyst}} = \oint M^* \, dS^*, \tag{22}$$

serves as a quantitative measure of this inertia. A larger $\mathcal{A}_{\text{hyst}}$ denotes a stronger internal persistence—an enhanced capacity of the system to maintain its previous alignment despite changing external or self-imposed conditions.

Hence, the emergence of hysteresis or bistability in $M^*(\lambda_{\text{fb}})$ is not a numerical artifact but a dynamical signature of self-stabilized memory: an internal feedback mechanism that embeds the system's history within its ongoing perceptual state. This phenomenology parallels the concept of magnetic, where internal feedback loops mediate both adaptability and stability within the self-regulating decision space. Quite interestingly, our proposition resonates with several experimental studies claiming a hysteresis effect [32–34] in the cognitive neuroscience studies.

4 Numerical Simulation Results

The coupled mean-field Bloch equations (Eqs. (9)–(11)) were integrated numerically for ensembles of $N = 200$ agents using a custom `Python`/`Numba` implementation. Each agent evolves through the fast perceptual variables (m_x^i, m_y^i, m_z^i) and the slow adaptive self variable s_i, coupled via the effective field $h_i^{\text{eff}}(t)$ that includes environmental drive, neighbor alignment, and self feedback. The time evolution was computed using a fourth-order Runge–Kutta (RK4) integrator implemented with in NUMBA, enabling efficient parallel execution across 48 CPU cores. Simulations were performed with a fixed time step Δt chosen to ensure numerical stability and accuracy equivalent to adaptive `solve_ivp` integration (typical $\Delta t \sim 0.01$–0.05). Initial Bloch vectors were drawn from small random perturbations around zero to break symmetry, while the self variables were initialized near $s_i \simeq 0$. The system was evolved up to $t = 100$ time units, with exactly 200 output steps recorded per trajectory. For each value of the feedback coupling λ_{fb}, full trajectories of $(m_x^i, m_y^i, m_z^i, s_i)$ were saved and analyzed to compute macroscopic observables: the mean transverse magnetization $M(t) = \langle |m_x + i m_y| \rangle$, the average self variable $S(t) = \langle s \rangle$, and their normalized covariance C_{MS} and phase lag Φ_{MS}. All computations were carried out deterministically with fixed random seeds to ensure reproducibility.

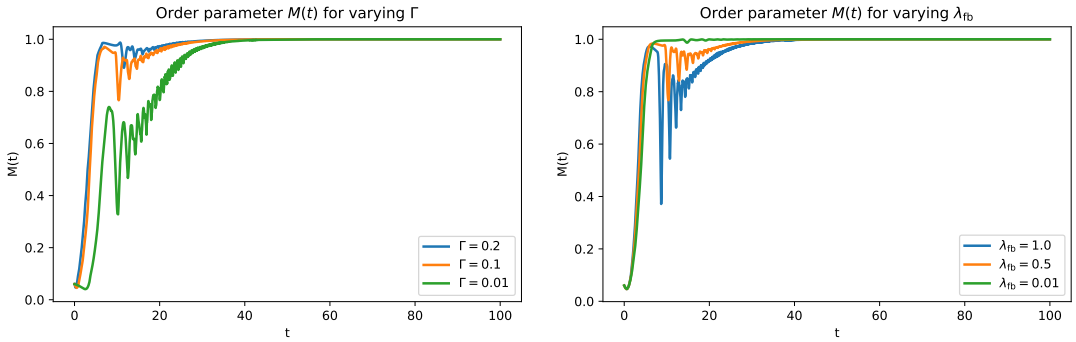

Figure 2: The temporal evolution of the collective order parameter or perceptual coherence $M(t)$ with the variations of Γ and λ_{fb}.

4.1 Temporal evolution of collective alignment.

Figure 2 illustrates the time evolution of the macroscopic order parameter $M(t) = \langle |m_x + im_y| \rangle$, which quantifies the instantaneous coherence of the perceptual subsystem. The left panel shows how $M(t)$ evolves for different precession rates Γ, while the right panel shows its dependence on the feedback strength λ_{fb}. For all cases, the order parameter exhibits an initial transient behavior characterized by oscillatory build-up of coherence, followed by relaxation to a near-saturated steady state ($M^* \approx 1$). Decreasing Γ (left panel) leads to slower and more strongly oscillatory convergence, indicating that transverse precession provides a stabilizing mechanism for collective alignment. In contrast, varying λ_{fb} (right panel) modulates the rate of coherence formation: weak feedback ($\lambda_{\text{fb}} \ll 1$) results in fast synchronization, whereas stronger λ_{fb} produces oscillatory buildup in $M(t)$. This is intuitive because with $\lambda_{\text{fb}} \ll 1$, self-regulation does not play any role in perceptual coherence.

The behavior of $M(t)$ in Figure 2 reveals two complementary roles of the system's key parameters. The transverse precession rate Γ controls how rapidly perceptual states explore phase space, effectively acting as a stabilizing "cognitive rotation" that suppresses excessive local correlations and enables smooth convergence to the collective mode. The feedback strength λ_{fb}, on the other hand, governs how strongly the slow self variable influences perceptual alignment, determining the speed and robustness of global ordering. Together, these parameters regulate the system's transition from disordered to coherent states, illustrating how self–perception coupling enables the emergence of synchronized perceptual behavior in a distributed ensemble.

Figure 3 shows how the normalized covariance C_{MS} and the phase lag Φ_{MS} between the macroscopic self variable $S(t)$ and the collective perceptual order parameter $M(t)$ vary as a function of the feedback strength λ_{fb}. At weak coupling ($\lambda_{\text{fb}} \approx 0$), both quantities are strongly negative, indicating that fluctuations in the self and perceptual subsystems are anticorrelated. An increase in perceptual coherence corresponds to a transient suppression of self-regulation. As λ_{fb} increases, C_{MS} and Φ_{MS} initially rise (becoming less negative), implying enhanced synchronization between self and perception. Beyond a critical feedback strength ($\lambda_{\text{fb}} \gtrsim 1$), both measures decrease again, showing a breakdown of coherent coupling as excessive feedback drives the system into a regime dominated by slow self-relaxation and delayed perceptual response. This nonmonotonic trend highlights a resonance-like regime of optimal feedback, where self–perception coupling achieves maximal mutual coordination before becoming dynamically overconstrained.

The joint variation of C_{MS} and Φ_{MS} in Figure 3 reveals how information transfer between the slow self and fast perceptual subsystems depends on the feedback strength λ_{fb}. As λ_{fb}

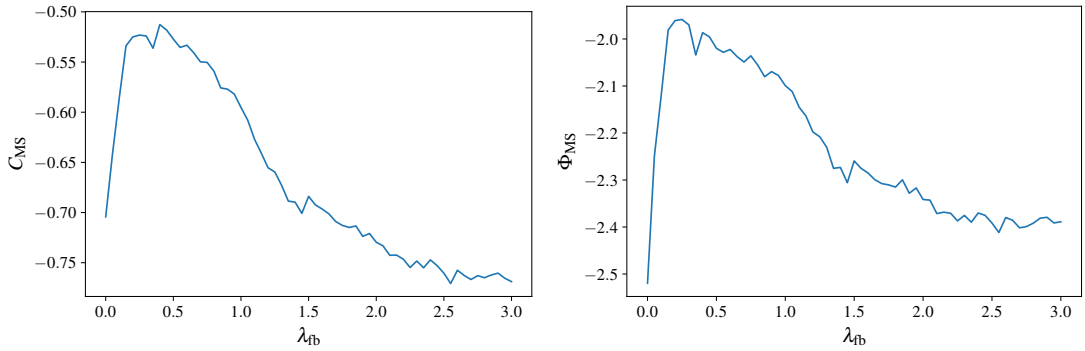

Figure 3: The evolution of normalized covariance C_{MS} and the phase lag Φ_{MS} between the macroscopic self variable $S(t)$ and the collective order parameter $M(t)$ with the variation of the feedback strength λ_{fb}.

increases, both quantities exhibit a nonmonotonic trend: moderate feedback enhances correlation and reduces the phase lag, indicating improved tracking of perceptual dynamics by the self variable. However, even at optimal coupling, Φ_{MS} remains negative, reflecting a persistent temporal delay in self adaptation relative to the perceptual field. At higher feedback strengths, both correlation and synchrony deteriorate, marking the onset of overcoupling and dynamic saturation. This regime-dependent behavior underscores that self–perception feedback functions as a finite-bandwidth regulator, balancing responsiveness and stability in collective adaptive dynamics.

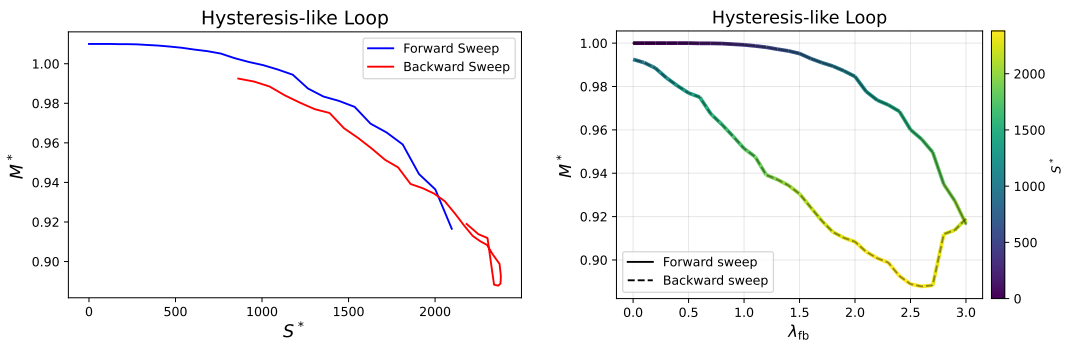

Figure 4: Hysteresis-like relationship between the equilibrium perceptual coherence M^* and the equilibrium self coherence S^* obtained from forward and backward sweeps of the feedback strength λ_{fb}. The loop illustrates memory-dependent transitions emerging from the self-perception feedback dynamics.

Figure 4 shows the emergence of a hysteresis-like loop between the equilibrium perceptual coherence M^* and the equilibrium self coherence S^*, obtained by sweeping the feedback coupling λ_{fb} forward and backward. The presence of a loop indicates a bistable regime in the coupled self–perception dynamics, in which the collective perceptual alignment does not follow the same trajectory when the feedback strength increases and decreases. During the forward sweep, the system remains in a high-alignment state ($M^* \simeq 1$) until a critical feedback threshold is crossed, beyond which coherence sharply decreases. In the reverse sweep, recovery occurs at a lower λ_{fb}, yielding a characteristic hysteresis loop. This asymmetry signifies the coexistence of multiple quasi-stable configurations of the perceptual and self subsystems, a hallmark of slow–fast interactions and memory-like effects in adaptive networks.

The hysteresis-like behavior illustrated in Figure 4 demonstrates that the self–perception feedback mechanism introduces an intrinsic form of collective memory into the system. Because the slow self variable integrates perceptual alignment over long timescales, the network retains traces of prior perceptual organization even as external or inter-agent coupling parameters change. Such path-dependent transitions are fundamental to adaptive decision-making and coordination in biological and cognitive collectives, where perception–action cycles operate under time-scale separation. In this sense, the loop reflects a macroscopic signature of cognitive hysteresis: the system's collective state depends not only on instantaneous inputs but also on its history of self–perception feedback. This mechanism provides a possible route for modeling persistence, inertia, or resilience in social, neural, and active-agent ensembles, linking microscopic feedback dynamics to emergent collective behavior.

The results presented here collectively reveal how adaptive feedback between perceptual coherence and slow self modulation can generate complex collective phenomena, including bistability, hysteresis, and memory-like persistence. While traditional models of active matter and alignment dynamics describe agents as following instantaneous interaction rules, the present framework incorporates an internal self variable that evolves on a slower timescale and integrates past perceptual states. This slow–fast coupling introduces effective non-Markovianity at the macroscopic level, endowing the system with history dependence and delayed relaxation, as captured by the hysteresis loops in Figure 4 and the correlation patterns in Figure 3. Moreover, the quantum-inspired formulation allows the coexistence of coherence (superposition-like states) and dissipation, providing a compact description of how uncertainty, attention, and feedback jointly shape emergent order.

Beyond reproducing well-known features such as synchronization and bistability, this model exposes the role of self–perception feedback strength as a control parameter for regulating collective cognition. Moderate coupling produces optimal coordination, whereas too strong a feedback leads to lag, instability, and coherence loss. This trade-off suggests a principle of adaptive regulation: effective coordination requires balancing self-stability with perceptual receptivity, a theme resonant with empirical findings in cognitive control and biological coordination.

5 Conclusion

We have introduced a quantum-inspired mean-field model of collective motion and cognition that unifies perception, self-regulation, and feedback within a single dynamical framework. By starting from a Gorini–Kossakowski–Sudarshan–Lindblad (GKSL) master equation and reducing it to coupled Bloch-type equations, we obtain an interpretable yet computationally tractable model of open-agent dynamics. This formulation bridges microscopic stochasticity and macroscopic order: fast perceptual variables capture coherence among alternatives, while slow self variables encode memory and volitional adaptation. The resulting dynamics exhibit bistability, hysteresis, and path-dependent transitions, which are the signatures of emergent collective intelligence rooted in the interplay of fast perceptual and slow self timescales.

Conceptually, this framework extends the language of quantum open systems to cognitive collectives, demonstrating that decoherence and feedback—traditionally studied in physical systems. It can serve as powerful metaphors and analytical tools in modeling attention, decision-making, and coordination. Unlike classical mean-field alignment models, the inclusion of the self degree of freedom endows the system with internal memory, enabling the emergence of hysteretic and adaptive responses to environmental change. The Bloch reduction provides a practical route for simulating large ensembles, translating abstract quantum dynamics

into interpretable differential equations that directly connect to measurable collective observables such as order parameters and phase correlations.

Looking forward, the model opens several promising directions. One avenue is to embed the current self–perception feedback scheme within spatially extended systems or networks with heterogeneous coupling topologies to explore the emergence of self-organized patterns, waves, and synchronization clusters. Another is to calibrate the model using empirical neural or behavioral data, linking the abstract self variable to measurable physiological indices such as neural oscillations, EEG microstates, or attentional dynamics. Ultimately, this approach aims to formulate a mathematically grounded yet biologically interpretable bridge between microscopic quantum-like representations of cognition and macroscopic emergent behavior in adaptive, self-organizing collectives.

References

[1] David JT Sumpter. *Collective animal behavior*. Princeton University Press, 2010.

[2] Tamás Vicsek and Anna Zafeiris. Collective motion. *Physics reports*, 517(3-4):71–140, 2012.

[3] Gabriel Popkin. The physics of life. *Nature*, 529(7584):16, 2016.

[4] Michele Ballerini, Nicola Cabibbo, Raphael Candelier, Andrea Cavagna, Evaristo Cisbani, Irene Giardina, Vivien Lecomte, Alberto Orlandi, Giorgio Parisi, Andrea Procaccini, et al. Interaction ruling animal collective behavior depends on topological rather than metric distance: Evidence from a field study. *Proceedings of the national academy of sciences*, 105(4):1232–1237, 2008.

[5] Sara Brin Rosenthal, Colin R Twomey, Andrew T Hartnett, Hai Shan Wu, and Iain D Couzin. Revealing the hidden networks of interaction in mobile animal groups allows prediction of complex behavioral contagion. *Proceedings of the National Academy of Sciences*, 112(15):4690–4695, 2015.

[6] Yi Ma, Eric Wai Ming Lee, Meng Shi, and Richard Kwok Kit Yuen. Spontaneous synchronization of motion in pedestrian crowds of different densities. *Nature human behaviour*, 5(4):447–457, 2021.

[7] Yann-Edwin Keta, Robert L Jack, and Ludovic Berthier. Disordered collective motion in dense assemblies of persistent particles. *Physical Review Letters*, 129(4):048002, 2022.

[8] Dante R Chialvo. Emergent complex neural dynamics. *Nature physics*, 6(10):744–750, 2010.

[9] Haitao Zhao, Hai Liu, Yiu-Wing Leung, and Xiaowen Chu. Self-adaptive collective motion of swarm robots. *IEEE Transactions on Automation Science and Engineering*, 15(4):1533–1545, 2018.

[10] Tamás Vicsek, András Czirók, Eshel Ben-Jacob, Inon Cohen, and Ofer Shochet. Novel type of phase transition in a system of self-driven particles. *Physical review letters*, 75(6):1226, 1995.

[11] John Toner and Yuhai Tu. Flocks, herds, and schools: A quantitative theory of flocking. *Physical review E*, 58(4):4828, 1998.

[12] John J Hopfield. Neural networks and physical systems with emergent collective computational abilities. *Proceedings of the national academy of sciences*, 79(8):2554–2558, 1982.

[13] Andrei Khrennikov. Quantum-like modeling of cognition. *Frontiers in Physics*, 3:77, 2015.

[14] Aghdas Meghdadi, Mohammad-R Akbarzadeh-T, and Kurosh Javidan. A quantum-like model for predicting human decisions in the entangled social systems. *IEEE Transactions on Cybernetics*, 52(7):5778–5788, 2022.

[15] Jennifer S Trueblood and Jerome R Busemeyer. A quantum probability account of order effects in inference. *Cognitive science*, 35(8):1518–1552, 2011.

[16] Andrei Khrennikov and Irina Basieva. Entanglement of observables: quantum conditional probability approach. *Foundations of Physics*, 53(5):84, 2023.

[17] Peter D Bruza, Zheng Wang, and Jerome R Busemeyer. Quantum cognition: a new theoretical approach to psychology. *Trends in cognitive sciences*, 19(7):383–393, 2015.

[18] Jan Broekaert, Irina Basieva, Pawel Blasiak, and Emmanuel M Pothos. Quantum-like dynamics applied to cognition: a consideration of available options. *Philosophical Transactions of the Royal Society A: Mathematical, Physical and Engineering Sciences*, 375(2106):20160387, 2017.

[19] Jyotiranjan Beuria, Mayank Chaurasiya, and Laxmidhar Behera. Collective motion from quantum-inspired dynamics in visual perception. *Proceedings of the Royal Society A*, 481(2321):20250489, 2025.

[20] Stuart Hameroff and Roger Penrose. Consciousness in the universe: A review of the 'orch or'theory. *Physics of life reviews*, 11(1):39–78, 2014.

[21] Fabio Bagarello, Irina Basieva, and Andrei Khrennikov. Quantum field inspired model of decision making: Asymptotic stabilization of belief state via interaction with surrounding mental environment. *Journal of Mathematical Psychology*, 82:159–168, 2018.

[22] Andrei Y Khrennikov. *Open quantum systems in biology, cognitive and social sciences*. Springer Nature, 2023.

[23] Shaun Gallagher. Philosophical conceptions of the self: implications for cognitive science. *Trends in cognitive sciences*, 4(1):14–21, 2000.

[24] Manos Tsakiris. The multisensory basis of the self: From body to identity to others. *Quarterly journal of experimental psychology*, 70(4):597–609, 2017.

[25] Georg Northoff and Felix Bermpohl. Cortical midline structures and the self. *Trends in cognitive sciences*, 8(3):102–107, 2004.

[26] F Schneider, Felix Bermpohl, A Heinzel, Michael Rotte, Martin Walter, C Tempelmann, Christina Wiebking, Henrik Dobrowolny, HJ Heinze, and Georg Northoff. The resting brain and our self: self-relatedness modulates resting state neural activity in cortical midline structures. *Neuroscience*, 157(1):120–131, 2008.

[27] Pengmin Qin and Georg Northoff. How is our self related to midline regions and the default-mode network? *Neuroimage*, 57(3):1221–1233, 2011.

[28] Christopher G Davey, Jesus Pujol, and Ben J Harrison. Mapping the self in the brain's default mode network. *NeuroImage*, 132:390–397, 2016.

[29] Peter Fransson. Spontaneous low-frequency bold signal fluctuations: An fmri investigation of the resting-state default mode of brain function hypothesis. *Human brain mapping*, 26(1):15–29, 2005.

[30] Vittorio Gorini, Andrzej Kossakowski, and Ennackal Chandy George Sudarshan. Completely positive dynamical semigroups of n-level systems. *Journal of Mathematical Physics*, 17(5):821–825, 1976.

[31] Goran Lindblad. On the generators of quantum dynamical semigroups. *Communications in mathematical physics*, 48(2):119–130, 1976.

[32] Caspar M Schwiedrzik, Christian C Ruff, Andreea Lazar, Frauke C Leitner, Wolf Singer, and Lucia Melloni. Untangling perceptual memory: Hysteresis and adaptation map into separate cortical networks. *Cerebral Cortex*, 24(5):1152–1164, 2014.

[33] Sonia Poltoratski and Frank Tong. Hysteresis in the dynamic perception of scenes and objects. *Journal of Experimental Psychology: General*, 143(5):1875, 2014.

[34] Jean-Remy Martin, Anne Kösem, and Virginie van Wassenhove. Hysteresis in audiovisual synchrony perception. *PloS one*, 10(3):e0119365, 2015.